

Single-Spin Beam Asymmetry in Semi-Exclusive Deep-Inelastic Electroproduction

Andrei Afanasev and C. E. Carlson [†]

Jefferson Lab, 12000 Jefferson Ave., Newport News, VA 23606, USA

[†]*Department of Physics, College of William and Mary, Williamsburg, VA 23187, USA*

Abstract. Recent measurements from Jefferson Lab show significant beam single spin asymmetries in deep inelastic scattering. The asymmetry is due to interference of longitudinal and transverse photoabsorption amplitudes which have different phases induced by the final-state interaction between the struck quark and the target spectators. We developed a dynamical model for a single-spin beam asymmetry in deep-inelastic scattering. Our results are consistent with the experimentally observed magnitude of this effect. We conclude that similar mechanisms involving quark orbital angular momentum ('Sivers effect') are responsible for both target and beam single-spin asymmetries.

Single-Spin Asymmetries (SSA) in semi-exclusive electroproduction reactions provide important new information about the nucleon spin structure [1, 2, 3]. Recent successful measurements of SSA in lepton production [4, 5] and anticipated experiments at Jefferson Lab after the 12-GeV energy upgrade stimulate a lot of interest in this subject.

One can relate SSA to the products of parton distribution and fragmentation functions, see Ref.[6] for review. In the quark-parton model, the origins of SSA can be attributed both to the time-reversal odd quark distribution, often called the 'Sivers effect' [1], and to the time-reversal odd fragmentation also known as 'Collins effect' [2]. Recently, Brodsky and collaborators [7] used a model to demonstrate that the target SSA can be generated at a leading twist level without time-reversal odd fragmentation. It led to the revision [8, 9] of time-reversal arguments, validating phenomenology with time-reversal odd parton distributions.

It has been known for a long time that single-spin polarization observables in particle scattering are caused by the spin-orbit interaction [10, 11]. SSA in deep-inelastic scattering should become a sensitive probe of the orbital angular momentum (OAM) of the participating quarks since SSA would simply vanish without contributions from both spin and OAM. It was demonstrated [7] that indeed OAM of quarks is crucial for describing target SSA.

In this work, we extend the calculation of SSA to the case of a polarized electron beam using the model that Ref.[7] used for the polarized target case. The model is reminiscent of model decomposition of the proton studied earlier in Ref.[12]. We demonstrate that a mechanism similar to Ref.[7] is also generating beam SSA of a magnitude compatible with experimental data. The considered mechanism does not require the Collins fragmentation function and therefore does not allow relation of the measured asymmetry to the quark distribution $e(x)$ introduced by Jaffe and Ji [3]. In this respect, our result for the beam SSA differs from analyses of Refs.[13, 14].

We calculate the beam SSA $A_{LU}^{\sin\phi}$ measured in the experiment and defined as

$$d\sigma \propto (1 + h_e A_{LU}^{\sin\phi} \sin\phi); \quad (1)$$

where $h_e = \pm 1$ indicates the electron beam helicity, and ϕ is the angle between the planes of electron scattering and hadron production. Following Ref.[7], we describe the deep-inelastic electroproduction process with a model of a spin 1/2 proton of mass M which is made from charged spin-1/2 and spin-0 constituents of masses m and λ , respectively (Fig.1). During the scattering, the virtual photon is absorbed by an active spin-1/2 parton, while the scalar diquark is used to describe the spectator system. The momentum of the knocked-out quark is set equal to the observed hadronic momentum. The proton-quark-diquark vertex function should be a solution to a bound-state equation, which we here simplify as a scalar vertex with a coupling parameter g .

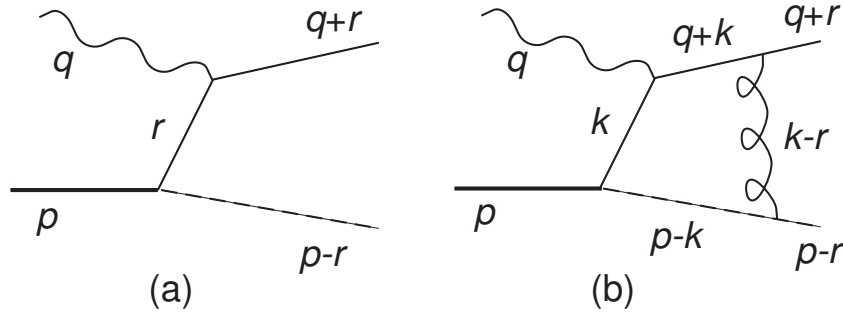


FIGURE 1. (a) Tree-level diagram and (b) Final-state gluon exchange.

The leading-order diagram Fig.1a alone produces zero asymmetry $A_{LU}^{\sin\phi}$, since its contribution to the scattering amplitude is purely real. The one-loop next-to-leading-order correction Fig.1b needs to be included in order to generate nonzero beam and target SSA. The loop diagram Fig.1b contribution is given by the formula

$$J_{\mu}^{NLO} = ie_q g C_F 4\pi\alpha_s \int \frac{d^4k}{(2\pi)^4} \frac{\bar{u}(q+r)\gamma_{\nu}(\not{q} + \not{k} + m)\gamma_{\mu}(\not{k} + m)(g_{\nu\tau})\not{2p} \not{k} \not{r}\gamma_{\tau}}{D_1 D_2 D_3 D_4}; \quad (2)$$

where $C_F = 4/3$ and D_i are denominators that come from the four propagators.

We calculate the contribution of the Fig.1 mechanism to the anti-symmetric part of the hadronic tensor defined by the imaginary part of the interference between Fig.1a and Fig.1b amplitudes. Cutkosky rules are used to calculate the absorptive part of the loop contribution, replacing two of the denominators D_i in Eq.(2) by the corresponding delta functions as follows:

$$\frac{1}{((q+k)^2 - m^2 + i\epsilon)((p-k)^2 - \lambda^2 + i\epsilon)} \rightarrow (2\pi i)^2 \delta((q+k)^2 - m^2) \delta((p-k)^2 - \lambda^2); \quad (3)$$

where m and λ are the masses of the quark and diquark, respectively. As a result, the 4-dimensional integration over the loop momentum in Eq.(2) is reduced to a 2-dimensional angular integration, making the result safe from ultraviolet divergence. The beam asymmetry is generated due to interference between absorption of longitudinal and

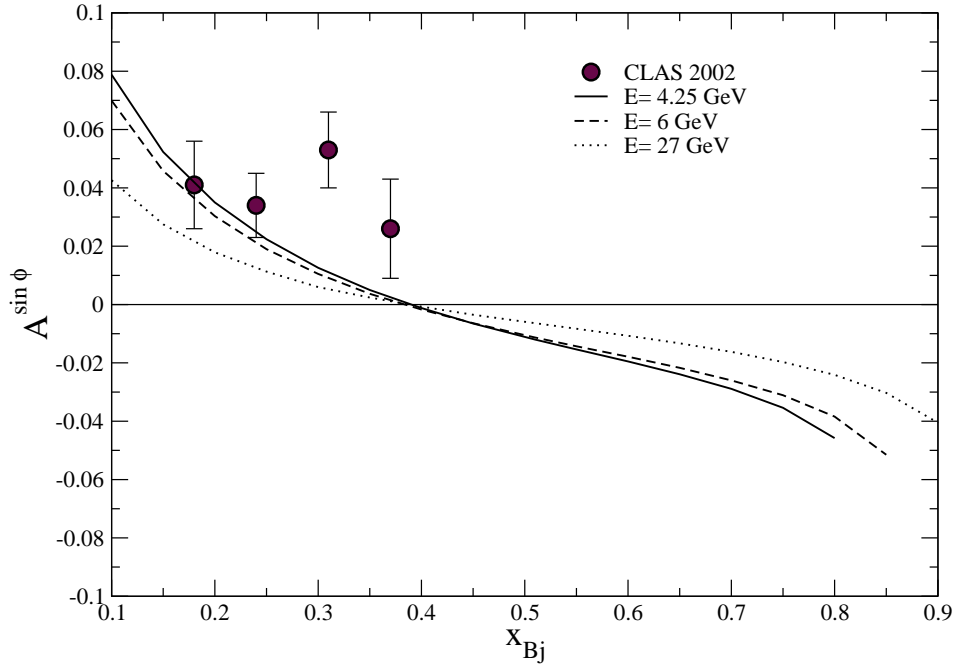


FIGURE 2. Beam SSA as a function of x_{Bj} for different beam energies at fixed $y=0.7$ and $r_T=0.4$ GeV/c. Data points are from Ref.[5] for the process $p(e;e^0\pi^+)X$.

transverse virtual photons (LT-interference) which acquire different phases as a result of final-state gluon exchange. In the scaling limit, the asymmetry is proportional to $r_T \frac{1}{\sqrt{Q^2}}$, where r_T is a transverse component of the final quark momentum. The factor $1/\sqrt{Q^2}$ points to the twist-three origin of this observable. The calculations were also performed in the light-cone gauge, producing the same results.

The amplitude Fig.1b is infrared-divergent as the momentum of the exchanged gluon approaches zero. However, the infrared-divergent terms exactly cancel at the level of observable asymmetry. The same spin-dependent mechanism reduces relative contribution of soft gluons to the integral Eq.(2). We also note that we neglected the loop correction to the unpolarized cross section, otherwise we would have to add real gluon bremsstrahlung or introduce an infrared cut-off to make the theory infrared-safe.

The results of our model for beam SSA is shown in Fig.2 for different beam energies as a function of Bjorken x_{Bj} . We used the values of the parameters $m = 0.3$ GeV, $\lambda = 0.8$ GeV and $\alpha_s = 0.3$. The value of the kinematic variable $y = 0.7$ and beam energies of 4.25 and 6 GeV are chosen to match the experimental conditions [5]. One can see that the prediction for beam SSA is consistent with its observed magnitude. For higher beam energies of 27 GeV relevant to the HERMES experiment [4] and fixed values of the kinematic variables $x_{Bj}; y$, the beam asymmetry is suppressed by about a factor of two, following the $1/\sqrt{Q^2}$ dependence. Our model predicts that the asymmetry changes its sign around $x = 0.5$, where no experimental data are available. Thus extension of experimental measurements to higher values of x can test validity of the proposed mechanism. Note that beam SSA calculated in a simplified model with scalar partons

is approximately constant as a function of x_{Bj} and equals about +0.08 for the 6-GeV kinematics of Fig.2.

Let us discuss the relation of the obtained results to the target SSA calculations of Ref.[7]. Target SSA are due to the T-odd observable $\mathcal{S}_p \cdot \boldsymbol{q} \cdot \boldsymbol{p}_h$ made from the proton polarization vector \mathcal{S}_p , the photon momentum \boldsymbol{q} , and the outgoing hadron's momentum \boldsymbol{p}_h . The essential ingredient of the model [7] is quark OAM in the initial nucleon state, so that the struck parton may have helicities both parallel and antiparallel to the nucleon helicity. Interference between transitions to different helicity states, supplemented by the phase difference due to final gluon exchange is the mechanism that generates the target SSA. Very similarly, beam SSA is due to the correlation $\mathcal{S}_\gamma \cdot \boldsymbol{q} \cdot \boldsymbol{p}$, where \mathcal{S}_γ is the virtual photon polarization. The beam SSA arises due to interference between longitudinal and transverse photoabsorption amplitudes, with the transverse momentum and phase differences generated by the same gluon-exchange mechanism as in the polarized target case. The quark OAM now unambiguously enters at the photon-parton level and the result does not depend on the quark OAM contribution to the nucleon light-cone wave function. Therefore, measurements of beam SSA are needed for adequate interpretation of target SSA measurements within a parton model. By analogy with the target asymmetry and in absence of T-odd fragmentation, we can view the considered mechanism as a *photon Sivers effect*, emphasizing the importance of this effect in polarized deep-inelastic scattering.

We acknowledge useful discussions with H. Avakian, S. Brodsky and D.S. Hwang. This work was supported by the US Department of Energy under contract DE-AC05-84ER40150. In addition, C.E.C. thanks NSF for support under grant PHY-0245056.

REFERENCES

1. D. W. Sivers, Phys. Rev. D **43**, 261 (1991).
2. J. C. Collins, Nucl. Phys. B **396**, 161 (1993) [arXiv:hep-ph/9208213].
3. R. L. Jaffe and X. D. Ji, Phys. Rev. Lett. **67**, 552 (1991); Nucl. Phys. B **375**, 527 (1992); P. J. Mulders and R. D. Tangerman, Nucl. Phys. B **461**, 197 (1996) [Erratum-ibid. B **484**, 538 (1997)] [arXiv:hep-ph/9510301].
4. A. Airapetian *et al.* [HERMES Collaboration], Phys. Rev. Lett. **84**, 4047 (2000); Phys. Rev. D **64**, 097101 (2001); Phys. Lett. B **562**, 182 (2003).
5. H. Avakian *et al.* [CLAS Collaboration], arXiv:hep-ex/0301005.
6. V. Barone, A. Drago and P. G. Ratcliffe, Phys. Rept. **359**, 1 (2002) [arXiv:hep-ph/0104283].
7. S. J. Brodsky, D. S. Hwang and I. Schmidt, Phys. Lett. B **530**, 99 (2002).
8. J. C. Collins, Phys. Lett. B **536**, 43 (2002).
9. A. V. Belitsky, X. Ji and F. Yuan, Nucl. Phys. B **656**, 165 (2003).
10. N. F. Mott, Proc. R. Soc. (London), **A124**, 425 (1929).
11. J. Schwinger, Phys. Rev. **69**, 681 (1946); *ibid.*, **73**, 407 (1948); L. Wolfenstein, *ibid.*, **75**, 1664 (1949); A. Simon, T. A. Welton, *ibid.*, **90**, 1036 (1953).
12. Z. F. Ezawa, Nuovo Cim. A **23**, 271 (1974); S. D. Drell and T. D. Lee, Phys. Rev. D **5**, 1738 (1972).
13. J. Levelt and P. J. Mulders, Phys. Lett. B **338**, 357 (1994); P. J. Mulders and M. Boglione, Nucl. Phys. A **666**, 257 (2000).
14. A. V. Efremov, K. Goeke and P. Schweitzer, Nucl. Phys. A **711**, 84 (2002); Phys. Rev. D **67**, 114014 (2003).